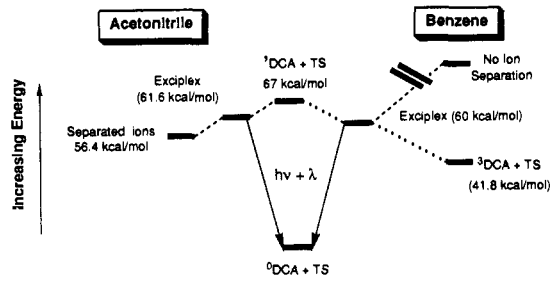

Figure 17. Relative energy diagram of emission and ion separation in CH_3CN and C_6H_6.

of this paper and the accompanying one demonstrate that oxygen directly quenches ^{1}DCA to produce $^1O_2$ in direct competition with other quenchers of ^{1}DCA. DMN quenches ^{1}DCA with a rate constant of 2.54×10^{10} s^{-1} in acetonitrile.[36] Under oxygen saturation ($\sim 10^{-2}$ M) and low ($\sim 10^{-3}$ M) DMN concentrations, oxygen can effectively compete for ^{1}DCA, and $^1O_2$ is produced with 146% efficiency (see the accompanying paper) from each interaction. The energy-transfer pathway to $^1O_2$ is probably dominant under Santamaria's reaction conditions.

Our mechanism can be summarized qualitatively in terms of the relative energy diagram shown in Figure 17. In benzene, the exciplex energy, obtained from the emission spectrum and reorganization energy of 0.3 eV,[19,37] is higher than that of the triplet, but ion-pair separation requires much higher energy, ruling out that pathway completely. Formation of ^{3}DCA competes with singlet exciplex emission. By contrast, in CH_3CN the exciplex (mainly CRIP[34]) has an energy above or near[34] the separated ions, whose relative energies are obtained from their redox potentials.[5,20,21] In Figure 17 we use λ_{max} of the exciplex emission to estimate the energy. However, in a closely related case, Gould et al.[34] report that the CRIP and separated ions have nearly the same energies. The polar solvent favors rapid ion separation and nearly, but not quite completely, suppresses exciplex formation and emission.

(37) Gould, I. R.; Ege, D.; Moser, J. E.; Farid, S. *J. Am. Chem. Soc.* **1990**, *112*, 4290-4301.

Summary

The results of this work show that the time-resolved 1270-nm $^1O_2$ luminescence can be used as an effective probe for the mechanism of photooxygenation reactions. If $\Phi_{^1O_2}$ is affected by substrate, it is necessary to look for substrate–sensitizer interactions and probe the system further. If only the $^1O_2$ lifetime is changed by substrate, a pure $^1O_2$ Type II mechanism is involved. This work also suggests that the production of $^1O_2$ from sensitizers can be subject to dramatic environmental effects and that the yield in homogeneous solution may not be predictive of that in more complex systems. This conclusion is particularly relevant for photodynamic therapy.

Acknowledgment. This work was supported by NSF Grants CHE86-11873 and CHE89-11916 and NIH Grant GM-20081. We thank Prof. N. Haegel (UCLA Dept. of Material Science and Engineering) for the use of spectroscopic equipment, and Dr. Samir Farid (Kodak) for measurement of the acetonitrile exciplex emission maximum and several very helpful discussions.

Registry No. TS, 103-30-0; DCA, 1217-45-4; O_2, 7782-44-7.

Electron-Transfer-Induced Valence Isomerization of 2,2′-Distyrylbiphenyl†

Arno Böhm,‡ Klaus Meerholz,§ Jürgen Heinze,*,§ and Klaus Müllen*,‡

Contribution from the Max-Planck-Institut für Polymerforschung, Ackermannweg 10, D-6500 Mainz, Germany, and Department of Physical Chemistry, University of Freiburg, Albert-Strasse 21, D-7800 Freiburg, Germany. *Received May 21, 1991*

Abstract: Upon chemical or electrochemical reduction, 2,2′-distyrylbiphenyl (**1**) rearranges into the "bis-benzylic" dianion, 3^{2-}, which can be either protonated to a 9,10-dibenzyl-9,10-dihydrophenanthrene or oxidatively coupled to a cyclobutane species. The mechanism of the electron-transfer-induced skeletal rearrangement is studied by product analysis and by cyclic voltammetry, and the results are compared with the outcome of the photolytic [2 + 2] cycloaddition.

1. Introduction

Over the last few years electron-transfer (ET) induced pericyclic reactions have become increasingly important in the syntheses of polycyclic compounds.[1-5] The increase in reactivity observed when going from the neutral to the corresponding ionic species allows one to bring about skeletal rearrangements for otherwise unreactive or thermolabile substrates.[1,5] In the chemical storage and directed release of solar energy, a key role has been attributed to electron-transfer-induced cycloadditions and valence isomerizations.[6-8]

While a number of publications have pointed out the advantages of an ionic reaction path in Diels–Alder reactions and other thermally allowed cyclization processes,[2,9] the potential of electron-transfer-induced [2 + 2] cycloadditions competing with the

† Reductive Transformations. 17. Part 16: Alexander, J.; Klabunde, K.-U.; Klärner, F.-G.; Lund, H.; Lund, T.; Müllen, K. *Chem. Ber.*, submitted for publication.

‡ Max-Planck-Institut.

§ University of Freiburg.

(1) Bellville, D. J.; Wirth, D. D.; Bauld, N. L. *J. Am. Chem. Soc.* **1981**, *103*, 718. Pabon, R. A.; Bellville, D. J.; Bauld, N. L. *J. Am. Chem. Soc.* **1983**, *105*, 5158. Harirchian, B.; Bauld, N. L. *Tetrahedron Lett.* **1987**, 927.
(2) Fox, M. A.; Hurst, J. R. *J. Am. Chem. Soc.* **1984**, *106*, 7626.
(3) Mlcoch, J.; Steckhan, E. *Tetrahedron Lett.* **1987**, 1081.
(4) Pattenden, G. K.; Robertson, G. M. *Tetrahedron Lett.* **1983**, 4617.
(5) Bauld, N. L.; Bellville, D. J.; Pabon, R.; Chelsky, R.; Green, G. *J. Am. Chem. Soc.* **1983**, *105*, 3584. Bauld, N. L.; Bellville, D. J.; Pabon, R. A.; Chelsky, R.; Green, G. *J. Am. Chem. Soc.* **1983**, *105*, 2378. Bauld, N. L.; Harirchian, B. *J. Am. Chem. Soc.* **1989**, *111*, 1826. Steckhan, E.; et al. *Synlett* **1990**, 275.
(6) Barber, R. A.; de Mayo, P.; Okada, K. *J. Chem. Soc., Chem. Commun.* **1982**, 1073.
(7) Draper, A. M.; de Mayo, P. *Tetrahedron Lett.* **1986**, 6157.
(8) Gassman, P. G.; Hershberger, J. W. *J. Org. Chem.* **1987**, *52*, 1337.
(9) Staley, S. W.; Heyn, A. S. *J. Am. Chem. Soc.* **1975**, *98*, 3852.

0002-7863/92/1514-688$03.00/0 © 1992 American Chemical Society

Scheme I. Thermochemistry and Photochemistry of **1** in Solution

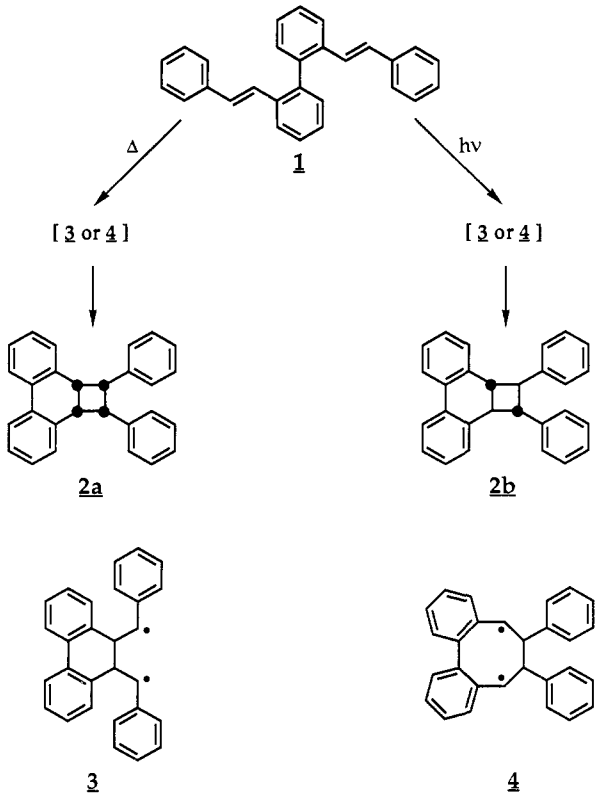

classical photochemical route is largely unexplored. However, this approach could be synthetically useful when providing access to cycloaddition products with configurations identical to those in the photochemical process[2,10,11] but under milder conditions.

It has long been known that 2,2'-distyrylbiphenyl (**1**) can be converted into the cyclobutane derivative **2** in a thermal as well as in a photochemical process.[12-14] The thermolysis stereoselectively leads to the all-cis cycloadduct **2a**, while photolysis transforms **1** almost completely into the all-trans isomer **2b** (Scheme I). For the formation of both products, a two-step biradical mechanism via intermediates, such as **3** or **4**, as well as a concerted process has been discussed.[13]

The radical monoanion, $\mathbf{1}^{\cdot-}$, prepared by alkali metal reduction of **1**, is stable at temperatures around −80 °C and can be identified by ESR spectroscopy.[15] Above −60 °C, however, it rearranges into a follow-up radical species, to which one can ascribe a dihydrophenanthrene framework. The question of whether in this case one is dealing with a cyclobutane system of type **2** could not be resolved from the ESR data. The fragmentation of this follow-up radical at temperatures above −25 °C into a phenanthrene and a stilbene fragment seemed to indicate the intermediate formation of a cyclobutane species, **2**.

In view of these preliminary results, a more intensive study of electron-transfer-induced valence isomerizations of **1** and a comparison with the corresponding photolytic and thermolytic reactions were appropriate. This work is concerned with the mechanism of an intramolecular valence isomerization of **1** under reductive conditions, as well as the synthetic usefulness of this reaction. This approach requires a combination of spectroscopic, preparative, and electrochemical methods.

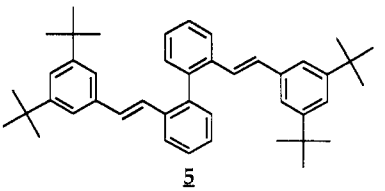

5

2. Results

2.1 Chemical Reduction. ESR spectroscopic monitoring of the reduction of **1** (deuterated tetrahydrofuran (THF-d_8), highly active potassium) revealed (i) the formation of radical monoanion $\mathbf{1}^{\cdot-}$ with an intact frame, (ii) its conversion into a follow-up radical with a dihydrophenanthrene structure, and (iii) its fragmentation into phenanthrene and stilbene radicals at higher temperatures. The attempt to obtain a more highly charged diamagnetic ion of **1** at −80 °C and to verify this spectroscopically by NMR failed because of the high tendency toward polymerization. This has already been found in similar cases.[2] Another serious drawback was the low solubility of the resulting anion salts in THF.

A sufficient solubility of the anions formed—allowing NMR spectroscopic control of the reduction—could be obtained by raising the reaction temperature to −25 °C. After a reduction time of 24 h, the very broad signals of a diamagnetic species could be detected. Prolonged metal contact gave rise to substantial amounts of polymeric material, and the dianions of phenanthrene and stilbene in an approximate ratio of 1:1.

On the other hand, in the reduction of the distyrylbiphenyl system **5**, which is substituted with *tert*-butyl groups to increase the solubility, using lithium or potassium at −25 °C, one obtained in both cases highly resolved spectra of the tetraanion salts $\mathbf{5}^{4-}/4Me^{+}$ without the formation of rearrangement or fragmentation products (Figure 1).

Reduction on a Preparative Scale. To gain information on the nature of the reactive intermediates, the parameters of the electron-transfer-induced rearrangement, such as solvent, temperature, reducing agent, amount of charge transfer, and time elapsed between reduction and quenching processes, had to be varied systematically. The reaction was terminated by transforming the resulting anions into neutral species with oxidizing or protonating reagents. From the structure of the protonation products, further conclusions could be drawn as to the structure of the ionic intermediates; on the other hand, a variation of the oxidizing reagent allowed for different chemical transformations of the anions.

All product mixtures were separated by column chromatography, and the products isolated were characterized by their NMR and mass spectra.

In a first series of experiments, the heterogeneous reduction of **1** at highly active potassium or lithium surfaces in THF (as solvent) was studied. The use of potassium as reducing agent allowed one to control the number of electrons transferred by the weight of the metal. However, this merely led to oligomeric or polymeric products. By using a large excess of lithium, the reduction times could be shortened and the tendency toward polymerization was decreased markedly. The reaction parameters used and the product distributions observed are summarized in Table I.

The reduction of **1** with lithium at −80 °C gave only substrate anions with an intact framework; subsequent warming up of the anion solution without metal contact to −25 °C led, after reoxidation with cadmium chloride, to 55% of a compound, to which structure **6** was assigned (see the Experimental Section).

The knowledge of the configuration of the benzyl substituents at positions 9 and 10 of the dihydrophenanthrene moiety is important for the formation of the DHP derivative **6**. A crystal structure analysis was not possible due to the microcrystalline character of the compound. The solution of the structural problem comes from the fact that **6** possesses two centers of chirality in positions 9 and 10. The cis configuration of the substituents leads to a meso form, and the trans configuration leads to a *d,l* form of the compound. Using HPLC with cellulose triacetate as the chiral stationary phase, separation of a sample of **6** into two

(10) Bauld, N. L.; Cessac, J. *J. Am. Chem. Soc.* **1977**, *99*, 23.
(11) Haselback, E.; Bally, T.; Lanyiova, Z. *Helv. Chim. Acta* **1979**, *62*, 577.
(12) Tulloch, C. D.; Kemp, W. *J. Chem. Soc. C* **1971**, 2824.
(13) Laarhoven, W. H.; Cuppen, Th. J. H. M. *J. Chem. Soc., Perkin Trans. 1* **1972**, 2074. op het Veld, P. H. G.; Laarhoven, W. H. *J. Chem. Soc., Perkin Trans. 2* **1977**, 268.
(14) Tol, A. J. W.; Laarhoven, W. H. *J. Org. Chem.* **1986**, *51*, 1663.
(15) Müllen, K.; Huber, W. *Helv. Chim. Acta* **1978**, *61*, 1310.

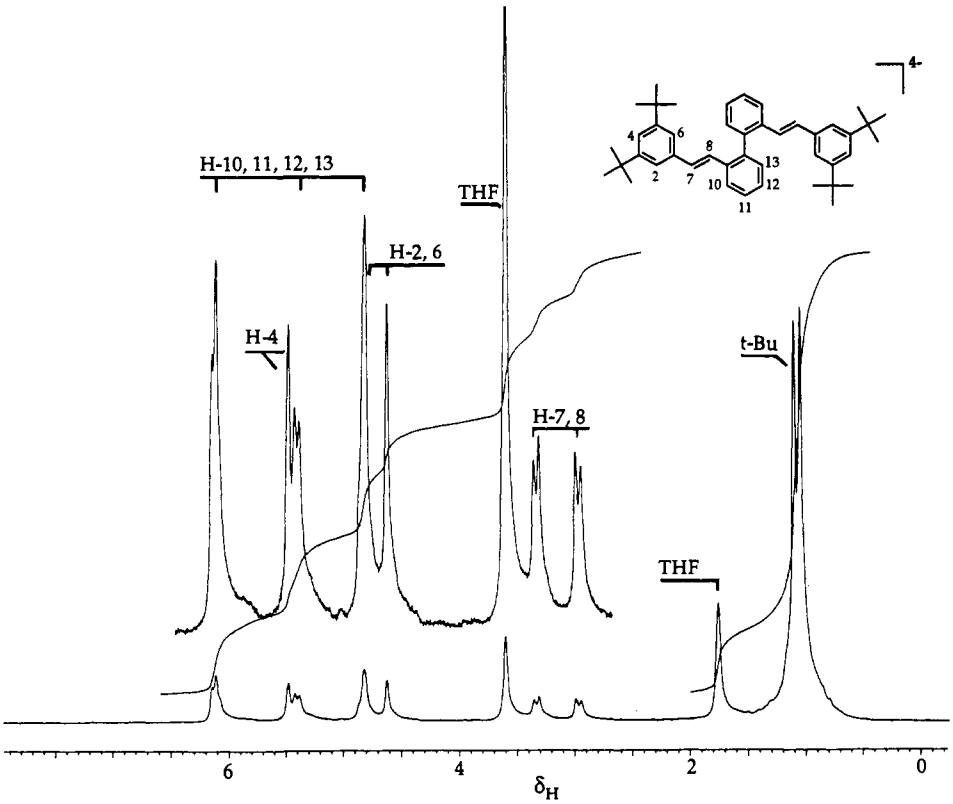

Figure 1. ^{1}H NMR spectrum of $5^{4-}/4Li^+$ in THF-d_8 (200 MHz, −25 °C).

Table I. Experimental Conditions and Product Distributions for the Heterogeneous Reduction of 1 and 5 with Lithium in THF

substrate	T_{red}[a] (°C)	t_{red}[a]	T_r[a] (°C)	t_r[a]	quenching agent	starting material (%)	dihydrophenanthrene derivative 6 (%)	phenanthrene/ stilbene (%)	oligomer/ polymer (%)[b]	run
1	−80	2.5 h	−25	4 days	$CdCl_2$		55		45	a
1	−80	17 h	−25	4 h	CH_2Br_2	22	27		50	b
1	−80	17 h	−25	4 h	$C_2H_4Br_2$	39	29		32	c
1	−80	17 h	−25	4 h	$C_3H_6Br_2$	3	24[c]		27	d
1	−50	33 days			$CdCl_2$		37	0.5/0.5	58	e
1	−50	35 days	−25	5 days	$CdCl_2$	6	23	7/12	52	f
1	−25	33 days			$CdCl_2$		18	20/30	32	g
1	−50	33 days			MeOH	7[d]	28		65	h
1	−50	33 days	−25	4 days	MeOH	9[d]	18	2/3	68	i
1	−25	33 days			MeOH	15[d]	10	6/23	47	j
5	−50	46 days			$CdCl_2$	51	8[e]		41	k
5	−25	46 days			$CdCl_2$	25	14[e]		61	l

[a] T_{red}: reduction temperature; t_{red}: duration of reduction; T_r: reaction temperature (see t_r); t_r: time elapsed between reduction and quenching process. [b] All polymer yields are given in mass %. [c] Additionally, the formation of 46% of an adduct between 6 and the quenching agent was observed. [d] Instead of starting material, the corresponding protonated species 10 was obtained in the course of the quenching reaction. [e] The corresponding *tert*-butyl-substituted derivative 8 was formed.

enantiomers was accomplished. Thereby, proof of the exclusive existence of the *d,l* form of 6 and of the trans configuration of the benzyl substituents at C_9 and C_{10} could be provided.

The formation of the intramolecular [2 + 2] cycloadduct 2 could not be observed. On the other hand, the product distribution was sensitive to the choice of quenching agents used (Table I, runs a–d; note, for example, the formation of adducts 7a and 7b with 1,3-dibromopropane as quenching agent).

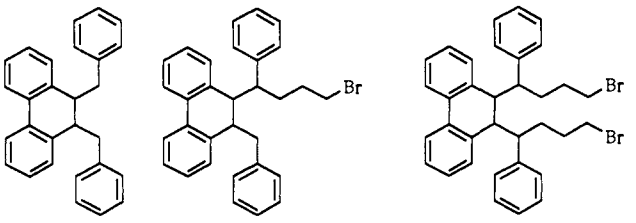

6 7a 7b

Increasing the reduction temperature to −50 °C and lengthening the reaction time led to a complete conversion of the starting material into 6 (37%) and an oligomer or polymer. Further raising the temperature to −25 °C decreased the yield of 6 to 18%, and the intramolecular [2 + 2] cycloaddition became the dominant reaction. The cyclobutane derivative formed was not stable under the reaction conditions. It immediately underwent a [2 + 2] cycloreversion to phenanthrene and stilbene, which could be isolated from the product mixture. The different yields of the two fragmentation products resulted from differences in the stability of the phenanthrene or stilbene anions formed during the course of the cycloreversion. A decomposition of the starting material into two stilbene fragments could be ruled out from the results of the redox studies on 5.

The following three experiments (Table I, runs h–j) should disclose how the product distribution was influenced by the equilibrium between slow reoxidation and fast protonation during the course of the quenching process. The product distributions determined for runs e–g differed from those in h–j. In the latter, the yield of starting material in the form of the protonated derivative 10 was distinctly higher while that of DHP derivative 6 lower than in the reactions e–g. An addition of both values gave nearly identical yields in all cases. The low yields of phenanthrene

Table II. Experimental Conditions and Product Distributions for the Homogeneous Reduction of **1** in Liquid Ammonia/THF

reducing agent	charge transferred (equiv)	T_{red}[a] (°C)	t_{red}[a]	T_r[a] (°C)	t_r[a]	quenching agent	substrate **1** (%)	protonated substrate (**10**) (%)	DHP derivative **6** (%)	run
potassium	1.5	−50	0.5 h			$CdCl_2$ NH_3	63	11	26	a
potassium	2	−50	2 h			$CdCl_2$ NH_3	57	19	24	b
potassium	6	−50	12 h			EtOH NH_3		19	81	c
potassium	2	−33	1.3 h			$CdCl_2$ NH_3	49	8	43	d
potassium	2	−80	0.2 h	−33 −25	1.5 h 5 days	$CdCl_2$ NH_3			100	e

[a] See footnote a of Table I.

and stilbene in reactions h–j can be explained by follow-up reactions after the protonation of the corresponding product anions.

The use of the *tert*-butyl-substituted species **5** under identical reaction conditions afforded the expected dihydrophenanthrene **8**, but with markedly lower yields (Table I, k and l). Formation of the [2 + 2] cycloadduct **9** or the corresponding cycloreversion products could not be observed even at higher temperatures.

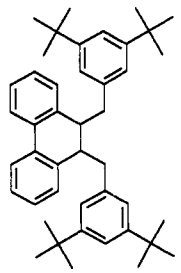

8

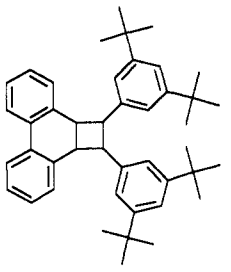

9

By using liquid ammonia as cosolvent and thereby homogeneous electron-transfer conditions, the observed reduction times were shortened to a few minutes and polymerization was no longer of importance (Table II).

In the product mixture, only starting material, dihydrophenanthrene derivative **6**, and—as a result of the acidity of the cosolvent—the tetrahydro derivative **10** were found. The yield of **6** increased markedly with the amount of metal used (from 26% with 1.5 equiv of potassium to 81% with 6 equiv). Parallel to this, the amount of **10** increased from 11 to 19%. Due to side reactions such as substrate protonation and potassium amide formation, the maximum attainable reaction time, t_{red}, depended strongly on the amount of metal used and could, thus, not be varied separately. By employing reaction temperatures higher than −50 °C, the amount of **6** could also be increased significantly. The protonation of the substrate to **10** was effectively suppressed. When the ammonia was evaporated from the solution shortly after electron transfer, a quantitative formation of **6** from **1** could be achieved (Table II, e).

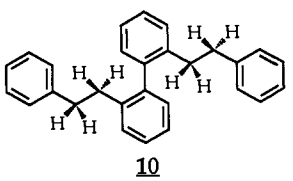

10

The use of mediating substances allows for a homogeneous electron transfer to the substrate even under aprotic conditions. For this purpose, compounds were required which form radical monoanions and dianions with redox potentials clearly below (mediator^0/mediator$^{\cdot-}$) or above (mediator$^{\cdot-}$/mediator^{2-}) the first two reduction steps of the substrate **1**. Under these provisions, exactly one electron per mediator molecule should be transferred to the substrate, and a reduction beyond the dianion could be prevented. In a first reaction step, the mediator chosen was reduced in THF to the appropriate redox stage using highly active lithium at −25 °C and—in a second step—was subsequently brought into contact with the substrate.

The results of these reactions are summarized in Table III, in which the same parameters as in the case of the heterogeneous alkali metal reduction (see Table I) were varied.

For anthracene as the electron-donating compound, the first reduction step of substrate **1** with −2.36 V (all of the following potentials were measured against Ag/AgCl; see next section) lies between that of the dianion (−2.55 V) and the radical monoanion of anthracene (−1.91 V). Thus, each anthracene dianion should transfer one electron to a substrate molecule under formation of the radical monoanion. No predictions could be made about a possible second electron transfer, since the second reduction stage of **1** with −2.55 V exactly corresponds to that of the anthracene dianion. 2,2'-Distyrylbiphenyl (**1**) reacted with 2 equiv of anthracene dianion to give, after reoxidation with cadmium chloride, besides 30% starting material, 2–7% of the dihydrophenanthrene derivative **6** and 10–13% of a compound to which structure **11** was assigned on the basis of NMR and MS evidence (see the Experimental Section).

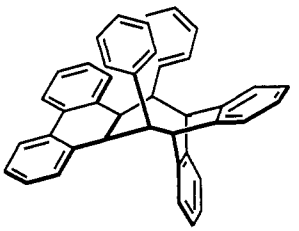

11

Under homogeneous conditions at high reaction temperatures, the cycloreversion products phenanthrene and stilbene were formed, but only when working with an insufficient amount of mediator and, thus, with radical monoanions of the substrates (Table III, b).

The reaction of 2,2'-distyrylbiphenyl (**1**) with 2 equiv of stilbene dianion ($E_{R\cdot-/R^{2-}}$ = −2.67 V) at −25 °C for 1 h, followed by oxidation with cadmium chloride, led to 30% 9,10-dibenzyl-9,10-dihydrophenanthrene (**6**) as the main product in addition to polymeric material. When methylene bromide or 1,2-dibromoethane was used in the quenching reaction, only starting material was obtained. Upon quenching with 1,3-dibromopropane, 28% of the mono- and diadducts **7a** and **7b** were formed.

The significance of the quenching agent becomes clear in the following example (Table III, f and g): the reoxidation using iodine led stereoselectively to the cyclobutane derivative **2b** with a yield of 25–28%, which can only be formed during the quenching reaction.

The last experiment of this series (Table III, h) shows that the previously observed low yield of dihydrophenanthrene derivative **6**, when using stilbene as a mediator, is a result of the quenching process; i.e., the fast protonation with methanol led to a quantitative isolation of the DHP derivative **6**.

In every experiment, the supposed precursor $\mathbf{3}^{2-}$ in the form of its dihydro derivative, but not the expected cyclobutane derivative **2**, could be isolated. The reoxidation with iodine is a

Table III. Experimental Conditions and Product Distributions for the Homogeneous Reduction of **1** in THF Using Appropriate Mediators

mediator	charge transferred (equiv)	T_r[a] (°C)	t_r[a]	quenching agent	mediator (%)	substrate (%)	adduct (%)	DHP derivative **6** (%)	cyclobutane derivative **2** (%)	phenanthrene/ stilbene (%)	oligomer/ polymer[b] (%)	run
A[a]	2	−50	18 h	$CdCl_2$	46	29	13[c]	7			25	a
A	1.1	−25	26 h	$CdCl_2$	60	9	2[c]	11		6	55	b
S[a]	2	−25	1 h	$CdCl_2$	75			30			52	c
S	2	−25	1 h	$C_3H_6Br_2$	70	11	28[d]	4			30	d
S	2	−25	24 h	$C_2H_4Br_2$	90	87					11	e
S	2	−25	24 h	I_2	96	55		7	28		7	f
S	2	−25	4 days	I_2	95	68			25		6	g
S	2	−25	4 days	MeOH	91			98			6	h

[a] T_r: reaction temperature; t_r: time of contact between mediator and substrate; A: anthracene; S: stilbene. [b] All polymer yields are given in mass %. [c] Adduct formation of **6** with the mediator to **11**. [d] Adduct formation of **6** with the quenching agent.

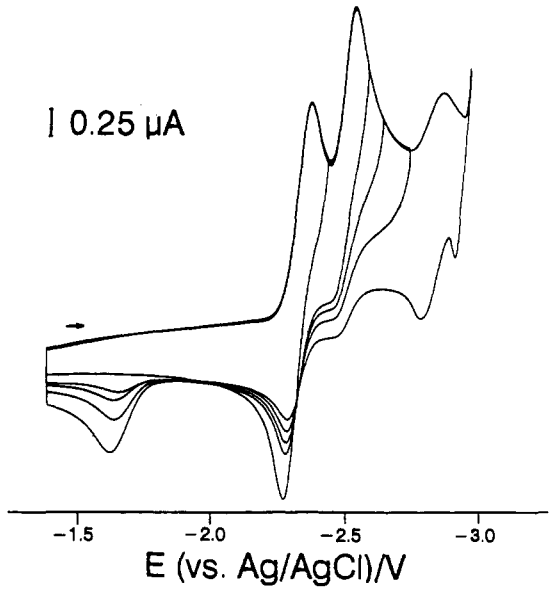

Figure 2. Cyclic voltammogram for the reduction of **1** in THF/$NaBPh_4$: v = 200 mV/s; T = −50 °C.

special case in this context, since the formation of **2** occurred only during the workup.

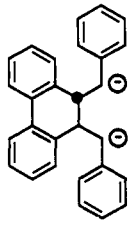

3^{2-}

2.2 Electrochemical Reduction. Within the scope of the preparative reduction experiments on 2,2′-distyrylbiphenyl (**1**), the formation of the products **6**, phenanthrene, stilbene, and, under special reoxidation conditions, **2** could be followed as a function of the reaction parameters. However, conclusions about the kinetics and the mechanism of the reaction were not possible. In this context, cyclic voltammetry (CV) appears as a powerful and complementary method of investigation. In recent years this method has proven its high reliability for the study of electron-transfer-induced valence isomerization.[16-19] By choosing the appropriate solvent and conducting salts, the reaction conditions of the preparative reduction could be simulated adequately. When comparing the electrochemical and preparative results, it must be taken into consideration, however, that in the case of the preparative reduction no supporting electrolyte salt is added to the solution. Thus, the ion-pair interaction of the anions formed with the alkali metal counterions will be greater than in the corresponding electrochemical experiment. The time scale of the CV experiment extends from a millisecond up to a minute, thereby covering a domain that is not accessible in the preparative experiments.

The first electrochemical reduction experiments were carried out in THF with lithium or sodium tetraphenylborate as supporting salts. Thus, the reaction conditions corresponded well to those of the alkali metal reductions in THF.

At low temperatures (−60 °C) and high sweep rates of 10 V/s or higher, **1** could be reversibly reduced into the trianion. The corresponding half-wave potentials are summarized in Table IV. While the first reduction step was chemically reversible, the reversibility of the second decreased when the sweep-rate was lowered. In the anodic sweep, the irreversible reoxidation wave

Table IV. Reduction Potentials of **1** and **5** and Their Follow-up Products[a]

R	electrolyte system	$E°_{R/R^{\cdot-}}$	$E°_{R^{\cdot-}/R^{2-}}$	$E°_{R^{2-}/R^{\cdot3-}}$	$E°_{R^{\cdot3-}/R^{4-}}$
1	I	−2.12	−2.21	−2.81	−3.13
	II	−2.36	−2.55	−2.86	
	III	−2.36	−2.58	−2.87	
	IV	−2.37	−2.56	−2.99	
	V	−2.34	−2.42	−2.92	−3.32
2b	I	−2.60	<−3.0[c]		
	II,III	−2.81			
3a	I		−1.63[b]	−2.98	
	II,III		−1.5 → −1.7[b]		
	IV		−1.80[b]		
	V		−1.86[b]	−3.18	
3b	I		−1.35[b]	−2.81	
	II,III				
	IV		−1.55[b]		
	V		−1.66[b]	−3.02	
5	I	−2.245	−2.37	−2.96	−3.25
	III	−2.40	−2.61	−2.84	
	IV	−2.40	−2.60	−3.01	
6	I	−2.68			
	II,III,IV,V	−2.90			
8	I	−2.80			
	III,IV	−2.91			
12	I				
	III,IV		−1.65[b]		

[a] Cyclic voltammetry was performed at a Pt electrode (d = 1 mm) with solutions 10^{-4}–10^{-3} M in substrate and various solvent–electrolyte systems: (I) DMA/0.1 M TBABr; (II) THF/0.1 M $LiBPh_4$; (III) THF/0.1 M $NaBPh_4$; (IV) THF/0.1 M $NaBPh_4$/15-Crown-5; (V) THF/$TBAPF_6$. All potentials are expressed in volts vs Ag/AgCl (for calibration, see the Experimental Section). Unless not noted differently the scan rate was 100 mV/s and the temperature −60 °C. For II and III the sweep rate was 1 V/s. [b] Anodic peak potential. [c] Cathodic peak potential.

(16) Kiesele, H.; Heinze, J. In *Organic Electrochemistry*; Lund, H., Ed.; Marcel Dekker: New York, 1991; p 331 ff.
(17) Kiesele, H. *Angew. Chem., Int. Ed. Engl.* **1983**, *21*, 254.
(18) Farnia, G. S.; Marcuzzi, F.; Melloni, G.; Sandona, G.; Zucca, M. V. *J. Am. Chem. Soc.* **1989**, *111*, 918.
(19) Farnia, S.; Sandona, G.; Marcuzzi, F.; Melloni, G. *J. Chem. Soc., Perkin Trans. 2* **1988**, 247.

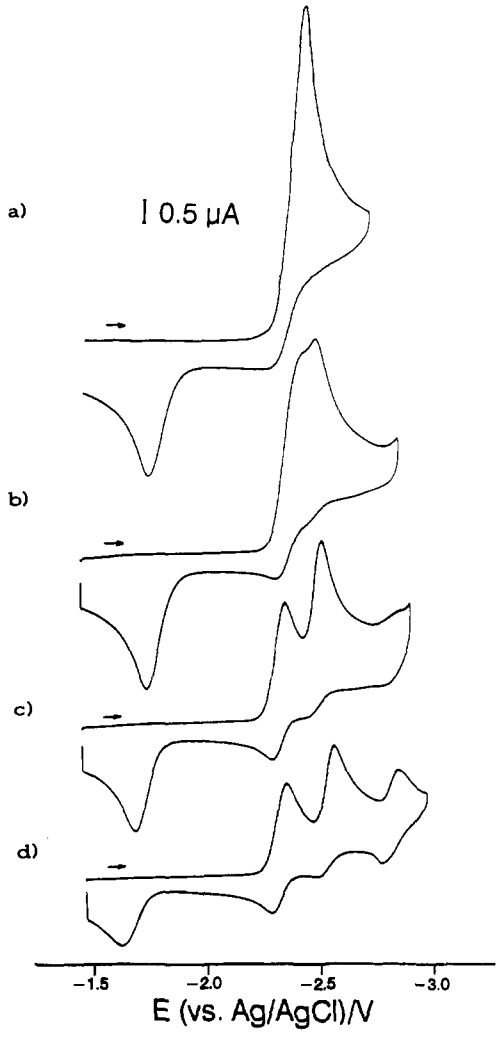

Figure 3. Cyclic voltammogram for the reduction of **1** in THF/$NaBPh_4$ (v = 100 mV/s): (a) T = 0 °C, (b) T = −20 °C, (c) T = −40 °C, (d) T = −60 °C.

of a follow-up product of the reacting dianion (Figure 2) was found between −1.5 and −1.7 V. In view of the formation of the DHP derivative **6** during the preparative reduction, this wave should correspond to its ionic precursor 3^{2-}. At the same time, the signal for the trianion formation of **1** diminished, because the amount of dianion 1^{2-}, which could be further reduced, decreased in the follow-up reaction.

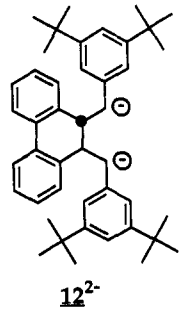

12^{2-}

When the temperature was raised, the chemical reaction of the dianion became faster. At the same time, the second reduction wave was shifted to more positive potentials due to increasing ion-pair effects (with decreasing dielectric constant of the medium, the solvation of the sodium ion decreases and the interaction increases). The intensity of the second peak decreased, while that of the first one increased. Finally, above −20 °C a single, overheightened reduction wave could be observed, corresponding to a formal two-electron reduction. In the reverse sweep, even the

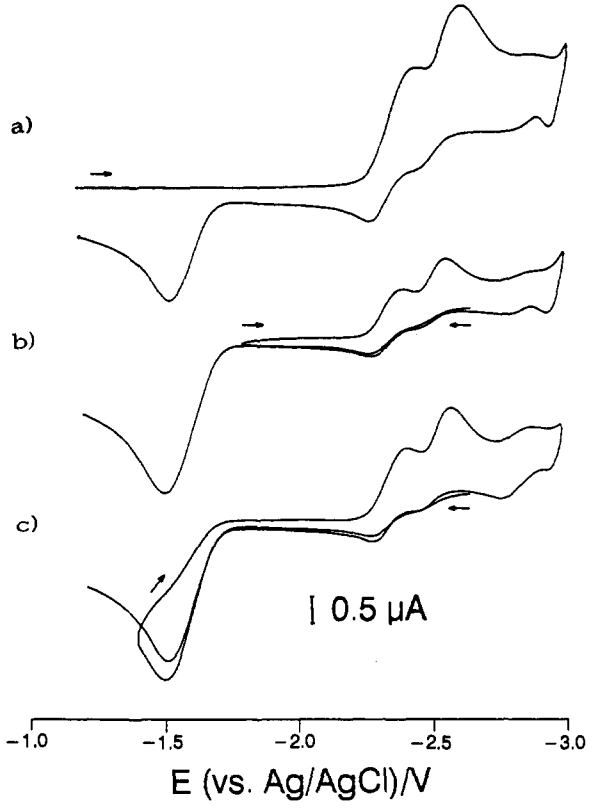

Figure 4. Cyclic voltammogram for the reduction of **1** in THF/$LiBPh_4$: v = 200 mV/s, T = −40 °C; (b, c) preelectrolysis at E = −2.70 V.

anodic wave of the first reduction step (Figure 3a,b) now disappeared. The type of follow-up product formed, however, did not change. When the sweep rate was increased, the anodic wave of the first reduction step again became increasingly reversible, and a situation analogous to the low-temperature experiment was observed.

Multisweep experiments in THF/$LiBPh_4$ revealed that 3^{2-}, after the reoxidation, gave mainly starting material **1**. When the potential sweep at −1.75 V was reversed before reaching the anodic reoxidation wave (E_{pa} = −1.55 V), only relatively small waves for the reduction of **1** into 1^{2-} (Figure 4b) were seen in the time-correlated cathodic sweep, whereas when the potential near −1.4 V was reversed, the reduction wave of the starting material significantly increased in intensity (Figure 4c). In addition, a new, relatively small signal corresponding to a reversible reduction at $E°$ = −2.81 V (Figure 4c) was observed. A later measurement, performed for an independently synthesized sample of **2b**, showed that here one was dealing with the reduction of the cyclobutane derivative.

For preparative isolation of the reoxidation products, a pulse experiment was carried out lasting 3 days (−30 °C, THF/$LiBPh_4$), in which 100 s on the dianion state at −2.7 V alternated with 1000 s at 0.0 V. Using this pulse technique, 3^{2-} was formed at −2.7 V without detectable polymer formation. In the next pulse, the reoxidation of the species occurred at −1.5 V. This process led to $3^{\cdot-}$ and then, in part, to $\mathbf{2b}^-$, which due to its extremely negative redox potential of −2.81 V was discharged immediately by homogeneous or heterogeneous electron transfer. In a competing reaction, 3^{2-} reacted by opening of the dihydrophenanthrene framework to **1**, which was re-reduced in the next cycle. Since the neutral cyclobutane derivative **2b**, once formed, could not take part in the following reduction processes, its concentration slowly increased in spite of unfavorable competing reactions. From the product mixture, 10% starting material, 60% DHP derivative **6**, and 30% cyclobutane derivative as all-trans isomer **2b** could be isolated. Thus, under these conditions the high stereoselectivity was retained.

Through the addition of 15-crown-5, which led to a complete complexation of the sodium ions, the behavior of substrate **1** during

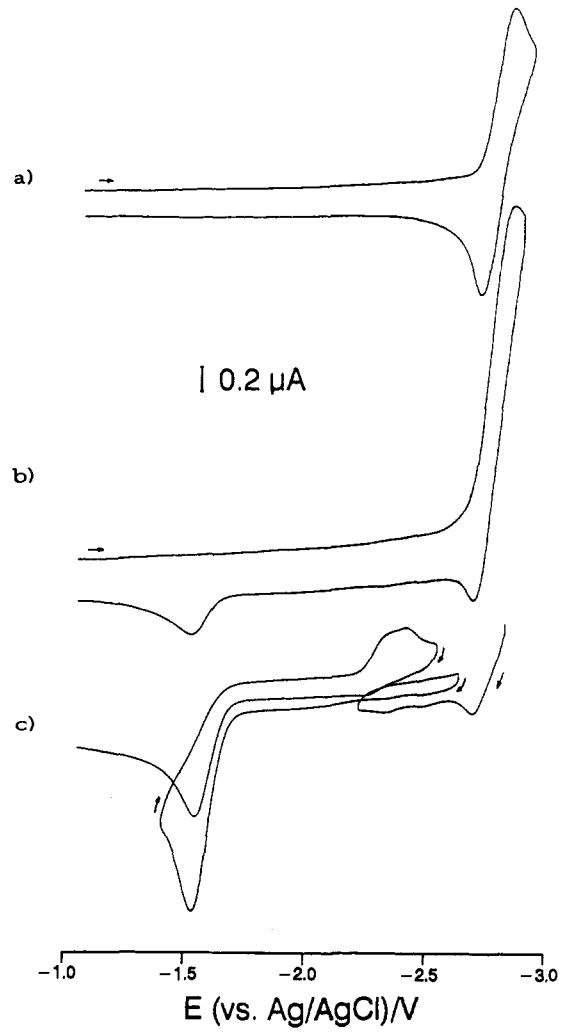

Figure 5. Cyclic voltammogram for the reduction of **2b** in THF/$LiBPh_4$ (v = 100 mV/s): (a) T = −60 °C, (b) T = −20 °C, (c) T = −20 °C; preelectrolysis at E = −2.90 V.

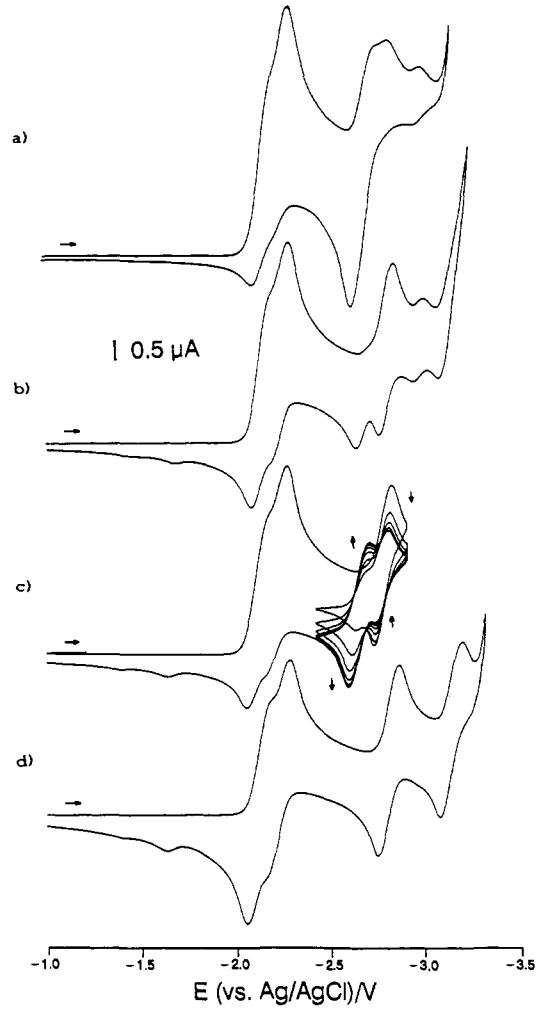

Figure 6. Cyclic voltammogram for the reduction of **1** in DMA/TBABr (v = 100 mV/s): (a) T = −20 °C, (b) and (c) T = −40 °C, (d) T = −60 °C.

the reduction in THF/$NaBPh_4$ changed drastically. Now, it could be reversibly charged to the trianion even under "mild" conditions (Table IV). At higher temperatures or slower sweep rates, follow-up products were observed in small amounts. These could be reoxidized irreversibly at E^a_{pa} = −1.55 V and E^b_{pa} = −1.80 V. In addition, a product was formed which could be reduced reversibly at −2.89 V. This species probably corresponded to the protonated DHP derivative **6**. The reduction potentials were now independent of temperature.

For reference purposes, on the cyclobutane derivative **2b** photochemically obtained from **1**, a cyclic voltammetric study was made of the tendency to fragment under reductive conditions. Below −60 °C, **2b** could be converted into the radical monoanion (Figure 5a) at −2.81 V. With increasing temperature, the reversibility of the reduction step decreased continuously, and the dependence of the cathodic peak current on the sweep rate that is typical of an ECE mechanism was observed. Again, follow-up products were formed which could be reoxidized at higher potentials (Figure 5b). The main product was identified from its reoxidation behavior as species $\mathbf{3}^{2-}$, already found in the reduction of **1**. The reoxidation of these species here also produced mainly **1**, detected in a time-correlated second cathodic sweep (Figure 5c).

The short-time electrolysis of **2b** at −3.0 V (T = −20 °C) provided another important finding: in the anodic potential sweep, three small waves of the same height were observed. These could be identified with the help of comparative measurements of the reoxidation of stilbene dianion (E^1_{pa} = −2.44 V, E^2_{pa} = −2.61 V) and of phenanthrene monoanion (E^3_{pa} = −2.83 V, appearing as a weak shoulder on the reverse peak of $\mathbf{2b}^{\cdot-}$/**2b**) (Figure 5c).

By using dimethylamine (DMA)[20] as the solvent and tetrabutylammonium bromide (TBABr) as the supporting electrolyte, the protolytic medium of the homogeneous reduction of **1** in liquid ammonia/THF could be simulated. At a temperature of −60 °C and a sweep rate of 500 mV/s, **1** could be reversibly reduced even to the tetraanion (Figure 6d). The redox potentials are listed in Table IV. With increasing temperature and decreasing sweep rate, the second reduction step became, as before, increasingly irreversible. In the reverse sweep at E^a_{pa} = −1.35 V and E^b_{pa} = −1.63 V, two relatively small waves with differing intensity ($i^a_{pa} < i^b_{pa}$) appeared which, similar to the measurements in THF/$NaBPh_4$, were due to the reoxidation of follow-up products formed out of $\mathbf{1}^{2-}$. Thereby, the trianion wave of **1** became less intense and, in the voltammograms, further waves due to electron-transfer reactions on the follow-up products were found at negative potentials (Figure 6).

One of these products, with a reversible step at $E°_{6/6^{\cdot-}}$ = −2.68 V and which dominated at high temperatures (−20 °C) and low sweep rates (Figure 6a), could be identified in an independent electrochemical reduction of an authentic sample as the dihydrophenanthrene derivative **6**. Its formation played a dominant role in the reduction experiments in liquid ammonia as well. A multisweep experiment between −2.5 and −3.0 V showed the transformation of the redox pair $\mathbf{1}^{2-}/\mathbf{1}^{\cdot3-}$ into the redox pair $\mathbf{6}/\mathbf{6}^{\cdot-}$. The isopotential points observed confirmed that the process takes place without side reactions within the time scale of the measurement (Figure 6c).

(20) Meerholz, K.; Heinze, J. *J. Am. Chem. Soc.* **1989**, *111*, 2325.

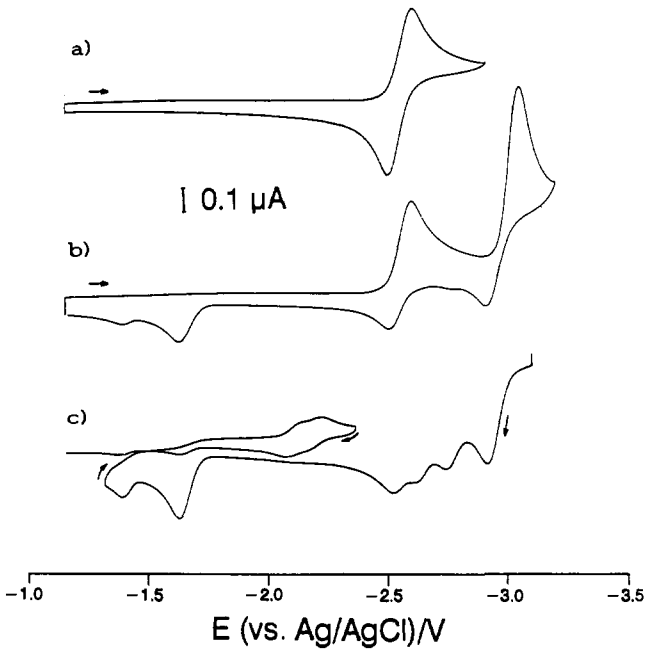

Figure 7. Cyclic voltammogram for the reduction of **2b** in DMA/TBABr: v = 100 mV/s, T = −60 °C; (c) preelectrolysis at E = −3.10 V.

A second reversible wave, also resulting from a follow-up reaction of 1^{2-}, was found at a potential of $E^{\circ,c}$ = −2.98 V.

Further information was provided by a series of experiments in which electrolysis was first carried out at the dianion stage of **1** (−2.4 V, 60 s), and single-sweep cyclic voltammograms, using the same sweep rate, were recorded in both the cathodic and anodic directions. In these, the peak-potential ratio, $i^a_{pa}/i^b_{pa} < 1$, increases significantly with decreasing sweep rate v and, in the reoxidation of both species, **1** was re-formed preferentially. Further, with increasing v, a peak-potential ratio of the waves at $E^{\circ,c}$ = −2.98 V and E^b_{pa} = −1.63 V of 1:2 was observed. This allowed the assignment of the reversible step at $E^{\circ,c}$ to the redox pair $3^{2-}/3^{\cdot 3-}$, whereby 3^{2-} was discharged to **1** at E^b_{pa} in an ECE reaction.

If, by contrast, electrolysis was carried out at the trianion stage of **1** (−2.9 V, 60 s), the significant increase of the waves at E^a_{pa}, E^b_{pa}, and $E^{\circ,c}$ in comparison with the electrolysis experiments at the dianion stage was observed. This points out that the mentioned follow-up process is fastened on the trianion stage.

The cyclobutane derivative **2b**, measured for reference purposes, could be reduced in DMA/TBABr at a potential $E^\circ_{2b/2b\cdot-}$ = −2.60 V into its monoanion in a chemically reversible process (Figure 7a). In comparison with the measurements in THF/Li(Na)BPh_4, a significant increase in the stability of the redox system was noted. The further reduction to the dianion at ca. −3.0 V, on the other hand, was completely irreversible. In the voltammograms, a cathodic wave appeared with twice the current height of the previous reversible step, indicating an ECE reaction under formation of a triply charged species (Figure 7b). This must be $3^{\cdot 3-}$, since at higher temperatures the formation of $6^{\cdot-}$ could be observed preferentially, while at lower temperatures this reaction path was negligible. The waves apparent as follow-up peaks at high sweep rates were mainly those already observed in the reduction of the parent compound **1** at E^b_{pa} and $E^{\circ,c}$. Using a longer measuring time scale, the waves at E^a_{pa} and a reversible step at $E^{\circ,d}$ = −2.81 V were observed (Figure 7b,c). The reoxidation waves for the monoanion and dianion of **1** were not found. This implied that the step $E^{\circ,d}$ could not correspond to the trianion step of **1**. The sum of the anodic peak currents for the reduction steps at $E^{\circ,c}$ and $E^{\circ,d}$ corresponded fairly exactly to the value of the monoanion step of **2b**. The time-correlated sweep showed that when the wave at E^a_{pa} as well as at E^b_{pa} was scanned the parent compound **1** was formed. As in the electrolysis of **1**, the peak-current ratios i^a_{pa}/i^b_{pa} and i^d_{pa}/i^c_{pa} increased with decreasing sweep rate.

After the electrolysis of **2** for 60 s at the dianion stage (−3.1 V; 3 charge equiv are transferred), during the anodic sweep at high sweep rates one observed the same peak-current ratio for the waves at E^a_{pa} and E^b_{pa} as for the redox steps at $E^{\circ,d}$ and $E^{\circ,c}$. This points toward the existence of two similar redox systems derived from structure type **3**.

Finally, we investigated the electrochemical behavior of **1** in THF/$TBAPF_6$ for studying the influence of solvent on the redox potentials and the follow-up processes. The redox potentials are listed in Table IV. In principle, the observations are very similar to those made in DMA/TBABr but, in addition to waves a–c, a reversible redox wave at $E^{\circ,d}$ appeared that was hidden in DMA by the $1^{2-}/1^{\cdot 3-}$ couple. At higher temperatures—in contrast to the experiments carried out with an alkali salt as the supporting electrolyte—a significantly increased amount of **6** was observed. Thus, the presence of the tetrabutylammonium ions seemed to be an important factor for the formation of this species. The polymer formation did not play any role in the time scale of the electrochemical experiments.

An exhaustive electrolysis of **1** in DMA/TBABr at −30 °C and a potential of −2.4 V led to the dihydrophenanthrene derivative **6** (85%). This agrees with the findings of the preparative reduction experiments in ammonia/THF. On changing to THF/$NaBPh_4$ (T = −10 °C, E = −2.7 V), polymer formation dominated (90%); in addition, 8% starting material and 2% **6** were found. In both cases, the entire charge transferred was lost.

In the investigation of the *tert*-butyl-substituted compound **5** it was found that, in analogy to **1**, in DMA/TBABr the compound could be charged up to the tetraanion in four reversible one-electron steps (Table IV). Only at high temperatures and slow sweep rates could small amounts of a single follow-up product be observed after passing the trianion stage. This product, probably the DHP derivative **8**, could be reversibly reduced at −2.8 V.

By analogy to **1**, in THF/$NaBPh_4$ **5** could be reversibly charged to the trianion at low temperatures and high sweep rates (Table IV). At higher temperatures and slower sweep rates, a follow-up product was again observed which could be irreversibly oxidized at a very positive potential (E_{pa} = −1.80 V). By analogy, it may be attributed to 12^{2-}. Thereby, **5** was re-formed exclusively. The follow-up reaction on the dianion stage, however, was significantly slower than in the case of the parent compound **1**. In addition, a reversible step at −2.91 V was observed, which could be attributed to the corresponding DHP derivative **8**. By the addition of 15-crown-5, follow-up reactions could be suppressed completely.

3. Discussion

The experimental data confirm that the heterogeneous or homogeneous reduction of 2,2'-distyrylbiphenyl (**1**) does not lead to the cyclobutane derivative **2** via an intramolecular [2 + 2] cycloaddition, as in the photo- or thermochemical reaction, but represents the starting point for a series of complex rearrangement and fragmentation processes. In the course of this, apart from phenanthrene and stilbene as fragmentation products of **2**, mainly *trans*-9,10-dibenzyl-9,10-dihydrophenanthrene (**6**) is formed. On the basis of the experimental results for the reduction of the parent compound **1** and the cyclobutane derivative **2b**, a general mechanism for the electron-transfer-induced valence isomerization of **1** is given in Scheme II.

At the start of the reduction, a polymerization reaction takes place at the radical anion level, as observed in similar cases.[2] The polymerization is inhibited when the radical anion $1^{\cdot-}$ rapidly undergoes further transformation. This conclusion is supported by the reduction experiments in THF using an excess of alkali metal (Table I), as well as by the homogeneous reduction experiments in liquid ammonia (Table II). In the voltammetric time scale, polymerization, being a relatively slow reaction, is never observed, and the first reduction step is even chemically reversible (see below). By contrast, the second reduction step, depending on the reaction conditions (temperature, electrolyte, sweep rate), is more or less irreversible. 1^{2-} is stable and can be charged further up to the tetraanion only at low temperatures (T < −60 °C). In all other cases, one observes the formation of a follow-up product

Scheme II

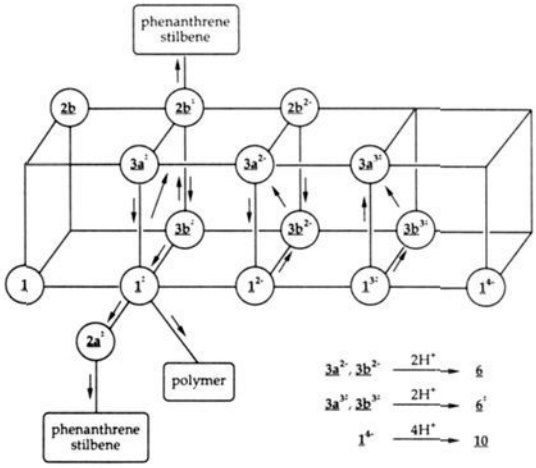

Scheme III

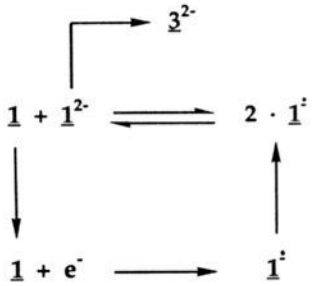

having a markedly more positive reduction potential. Judging from the results of the preparative experiments in which the dihydrophenanthrene derivative **6** is formed, the follow-up product observed in the CV experiment must be the diionic precursor of **6**, i.e., 3^{2-}. It is known from related examples that such benzyl anions possess a very positive redox potential.[21] Also remarkable is the high stereoselectivity of this reaction: the isomer with trans-configurated benzyl substituents is formed exclusively. The rearrangement of 1^{2-} into 3^{2-} is accelerated at higher temperatures and is favored by ion-pair interaction. The irreversibility of the radical anion formation from **1** observed in the voltammetric experiments above −20 °C is an artifact pointing toward an ECE mechanism. In reality, however, it must be attributed to a special EEC(DISP) mechanism (Scheme III) which, until now, has not been described in the literature.

Due to the ion-pair effect, the thermodynamic stability of $1^{\bullet-}$ ($E^\circ_2 - E^\circ_1 \rightarrow 0$) decreases with increasing temperature. Since at the same time 1^{2-} reacts faster, the disproportionation reaction, forming **1** and 1^{2-}, is favored kinetically as well as thermodynamically. This stipulates, first, that the concentration of $1^{\bullet-}$ decreases in the diffusion layer in front of the electrode and thus, in the reverse sweep, is no longer accessible for reoxidation. As a result, the voltammogram appears irreversible with respect to the first redox step, in spite of the fact that $1^{\bullet-}$ is completely stable within the time scale of the experiment. On the other hand, starting material **1** is re-formed by disproportionation. It is immediately charged again on the electrode, so that the heterogeneous charge transfer occurs mainly through the redox couple $1/1^{\bullet-}$. Thus, a formal two-electron transfer is observed experimentally. Simulation calculations corroborate this methodic concept.[22]

Quantitative data about the rate constant of the follow-up reaction of 1^{2-} to 3^{2-} are available from simulations using the working curves.[23] In THF/$NaBPh_4$ at −40 °C (−20 °C), one obtains a value of 0.2 s^{-1} (0.8 s^{-1}) for the first-order rate constants, while in DMA/TBABr they can be estimated at 0.04 s^{-1} (0.2 s^{-1}).

If only weak ion-pair interactions are present, one observes two follow-up products of the reacting dianion 1^{2-}, both of which can be reduced further to the trianion.

Since the chemical analysis of the products formed reveals only the isomer of **6** with trans-configurated benzyl substituents, the formation of an isomer with the cis configuration or the dibenzocyclooctane derivative **4** as possible explanations for the second peak can be excluded. On the other hand, the assumption that the follow-up products are two conformers of the trans-configurated species 3^{2-}, that is $\mathbf{3a}^{2-}$ and $\mathbf{3b}^{2-}$, is consistent with all voltammetric examinations. In $\mathbf{3a}^{2-}$, the rotation of the benzyl units is not hindered, and the two charges are at the greatest possible distance from each other. In $\mathbf{3b}^{2-}$, the benzyl substituents are nearly fixed, and the two charges are localized closer together than in $\mathbf{3a}^{2-}$. Thus, $\mathbf{3a}^{2-}$ is the thermodynamically favored conformation, and oxidation takes place at a more positive potential than in the case of $\mathbf{3b}^{2-}$. The further reduction of both species to the corresponding trianions occurs at the biphenyl moiety, since the two charges already present are localized in the benzyl units. The trianion formation of $\mathbf{3b}^{2-}$ takes place at a more negative potential, since here the benzyl units are located closer to the central biphenyl segment, making their charging more difficult for electrostatic reasons.

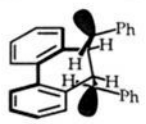

$\mathbf{3a}^{2-}$

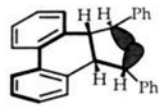

$\mathbf{3b}^{2-}$

The electrochemical measurements show that the formation of the thermodynamically less stable follow-up product, $\mathbf{3b}^{2-}$, from 1^{2-} is preferred kinetically and that it subsequently rearranges into $\mathbf{3a}^{2-}$. The same is true for the formation of 3^{2-} from $\mathbf{2b}^{\bullet-}$ or $\mathbf{2b}^{2-}$; here, initially only the conformer $\mathbf{3b}^{2-}$ is formed. An unambiguous statement about the position of the equilibrium between the two conformers is not possible. In the presence of alkali ions, however, it lies completely on the side of $\mathbf{3b}^{2-}$, since ion-pair interactions between the alkali cation and both charged benzyl substituents are possible at the same time, e.g., by forming bridged structures. The stereoselective formation of **2b** takes place through reoxidation of $\mathbf{3b}^{2-}$ only, while the protonation of both conformers leads to **6**. The rate constant for the protonation in DMA at −40 °C (−20 °C) is determined to be 0.01 s^{-1} (0.6 s^{-1}).

A similar ion-pair effect is also found in the case of the anions $1^{\bullet-}$ and 1^{2-} with intact frames. If measurements are carried out in the presence of TBA^+ ions—conditions under which only weak Coulombic interactions occur—the potential difference between the first and second reduction waves amounts to about 90 mV in DMA as well as in THF. By contrast, in the presence of alkali ions a potential separation of up to 220 mV can be observed, indicating a stronger Coulombic repulsion of the two excess charges. This behavior can be explained in the first case by a decoupling of the electroactive subunits resulting from a twist about the central single bond in the biphenyl unit, while the second finding points toward the formation of bridged contact ion pairs.

At the trianion stage, the same rearrangement as at the dianion level takes place. In the presence of alkali ions any contribution to the overall reaction is insignificant, because the rearrangement already takes place very quickly at the dianion stage. If, on the other hand, there is no ion-pair interaction, one observes the increased formation of $\mathbf{3a}^{\bullet3-}$ and $\mathbf{3b}^{\bullet3-}$ or $\mathbf{6}^{\bullet-}$ at the trianion stage, while the rearrangement at the dianion stage proceeds rather slowly. In this case the homogeneous rate constant for the reaction of $1^{\bullet3-}$ to $3^{\bullet3-}$ in DMA at −40 °C can be estimated as 0.2 s^{-1}.

For electrostatic reasons, the tetraanion of the substrate **1** is inert to any kind of rearrangement. This view is supported by

(21) Peters, D. G. In *Organic Electrochemistry*; Lund, H., Ed.; Marcel Dekker: New York, 1991; p 361 ff.
(22) Heinze, J. Manuscript in preparation.
(23) Störzbach, M.; Heinze, J. *J. Electroanal. Chem.*, in press.

the reversibility of the fourth redox step in the cyclic voltammogram. In the case of a fast protonation, it can be intercepted in its frame-intact form as tetrahydro derivative **10** (Table I, h–j).

For the reoxidation of 3^{2-} under all experimental conditions, a single anodic wave was observed. It proves that the reoxidation takes place via an ECE mechanism and not via an EEC mechanism. That is, the chemical reaction takes place at the radical anion stage. Principally, the instable monoanions **3** formed during the first step can react either through bond cleavage to the radical monoanion of the parent compound **1** or through bond formation to that of the cyclobutane derivative **2b** (only possible with **3b**). $\mathbf{1}^{\cdot-}$ as well as $\mathbf{2b}^{\cdot-}$ possesses a more negative reduction potential, and both relinquish their electrons immediately. Bond breaking in $\mathbf{3}^{\cdot-}$ is generally faster than bond formation. On the other hand, in the preparative experiments the re-formation of the starting material is observed when the reoxidation is carried out at low temperatures and aprotic conditions (Table I, b and c; Table III, e–g). Raising the temperature and increasing the interionic interactions favor the ring closure to **2b**. If the reoxidation of the system is performed slowly, as seen clearly in the chemical workup with iodine (Table III, f and g), both processes show similar rate constants; **2b** as well as **6** can be isolated from the product mixture. Alternatively, **2b** can be electrochemically enriched in the reaction mixture through a multistep experiment (see the electrochemical section).

From the electrochemical investigations of the cyclobutane derivative **2b**, it can be concluded that the corresponding radical monoanion $\mathbf{2b}^{\cdot-}$ is only stable under extreme conditions. Normally, it decays under the uptake of another electron via $\mathbf{3b}^{\cdot-}$ to the dianion $\mathbf{3b}^{2-}$ and, to a much lesser extent, into the cleavage products phenanthrene (monoanion) and stilbene (dianion). The latter can only be observed in THF/Li(Na)BPh_4. Here, marked influence of the counterion is also seen: the stronger the ion-pair effect, the less stable the radical monoanion.

The dianion of **2b** is extremely unstable. A rapid bond opening to $\mathbf{3b}^{2-}$ is seen, which in turn can accept a third electron and then rearrange into $\mathbf{3a}^{\cdot 3-}$. From the fact that no dianions of **1** are found in the solution, the formation of 3^{2-} from 1^{2-} must take place irreversibly or the equilibrium between both species lies far on the side of 3^{2-}. At the dianion stage no formation of phenanthrene and stilbene occurs. The pronounced selectivity of the bond breaking in the cyclobutane ring has already been observed in the photochemical or electron-transfer-induced (via $\mathbf{2b}^{\cdot+}$ as intermediate) [2 + 2] cycloreversion of **2b**.[24,25]

The results of the cyclic voltammetric studies on **1** and the appearance of the dihydrophenanthrene derivative **6** as the main product in the preparative reductions show that the reactive species in the observed rearrangement is the dianion 1^{2-} and not the radical monoanion $\mathbf{1}^{\cdot-}$. On this premise, the absence of **2** in the product mixture (except the cyclobutane derivative formed during the reoxidation with iodine) is understandable. The repulsive electrostatic forces appearing during an approach of the benzylic carbons make bond closure and cyclobutane formation impossible. Besides, as already described, **2b** cannot be transformed into a dianion. Decomposition already takes place at the monoanion stage.

On the other hand, the results of the preparative reduction show that phenanthrene and stilbene are formed at high reaction temperatures, which can only be explained by an intermediate formation of **2** in the reaction mixture. It is plausible that **2**—as in the reoxidation of 3^{2-}—should be formed from the radical anion of **1**, however, very slowly and in competition with an intermolecular polymerization reaction. Both processes are not observed on the voltammetric time scale. At high temperatures, four-ring formation becomes faster. The corresponding product **2**, however, is not stable under these conditions and decomposes either by re-forming the starting material, which can again take part in the reduction process, or ultimately by fragmentation into phenanthrene and stilbene, which are enriched during the course of the reaction. It could be shown[25] that the cation radical induced [2 + 2] cycloaddition of **1** leads exclusively to the all-cis-configurated cyclobutane derivative **2a**, which can then be transformed photochemically into phenanthrene and stilbene.[24,25] If one takes into consideration the topochemical selection rules for electrocyclic reactions of spin doublets put forth by Bauld,[10] an analogous reaction sequence should exist at the stage of the radical anion. This means that, besides $\mathbf{2b}^{\cdot-}$ and depending on the reaction conditions, notable amounts of $\mathbf{2a}^{\cdot-}$ should be formed, which decompose immediately into phenanthrene and stilbene.

The type and duration of the quenching process can also affect the product distribution in the preparative experiments. First of all, in the case of the heterogeneous reduction with a large excess of alkali metal, a certain amount of the starting material is reduced beyond the trianion stage before it can enter the follow-up reaction sequence. These highly charged substrate anions are inert against any kind of rearrangement for electrostatic reasons. In the case of a fast protonation, they can be quenched to a tetrahydro derivative, **10**, of the starting material (Table I, h–j). In the case of a slower reoxidation, they pass through the lower anion stages again and can, at that point, undergo valence isomerizations.

By changing from oxidative to protic workup conditions, the ratio between **1**, **6**, and **2** can be controlled. If no proton sources are present, the reaction of 3^{2-} leads to **1** or **2b** (see Table III, f and g). If proton donors are present in the reaction mixture, **6** is formed exclusively. In the case of a reoxidation process taking place at the same time—as it can be observed when using methylene bromide or 1,2-dibromoethane as the quenching reagent—the monoanion $\mathbf{3}^{\cdot-}$ also gets involved in the reaction and radical protonation becomes more important.

The *tert*-butyl-substituted derivative **5** can also be transformed into the corresponding dihydrophenanthrene **8** in accordance with the mechanism stipulated above. The bond formation during the conversion of 5^{2-} into the dianion 12^{2-} (similar to 3^{2-}) takes place significantly more slowly than in the unsubstituted parent compound **1**. This is supported by the lower yields of **8** in the preparative reductions, as well as by the greater reversibility of the second reduction step in the electrochemical investigations. On the other hand, the protonation of 12^{2-} to **8** takes place much faster than the protonation of 3^{2-}. This can be attributed to an increased basicity of the dianion due to the inductive effect of the *tert*-butyl groups. Since the second bond formation to the cyclobutane system is sterically hindered, even at high temperatures neither the formation of the [2 + 2] cycloadduct **9** nor of the corresponding cycloreversion products can be observed.

4. Conclusion

It has been shown that upon reduction 2,2'-distyrylbiphenyl (**1**) undergoes a complex rearrangement sequence which, depending on the conditions of the final quenching step, leads to 9,10-dibenzyl-9,10-dihydrophenanthrene (**6**) or to the corresponding cyclobutane derivative **2b**. The mechanism of the skeletal rearrangement and its dependence on various reaction parameters have been elucidated by using an appropriate combination of product analysis and cyclic voltammetry.

The homogeneous reduction of **1** and related compounds such as **5** in ammonia/THF provides a simple synthetic access to a series of new 9,10-dibenzyl-substituted 9,10-dihydrophenanthrenes. By an appropriate choice of the reaction conditions, a quantitative conversion of **1** into **6** occurs within a few hours. Only the product containing trans-configurated benzyl units in the 9,10-positions is formed in a stereoselective process. Since this stereoselectivity depends primarily on the geometry of the starting material, the stereochemical course of this reaction in similar systems with different molecular topology cannot be predicted as yet. Our work will focus on this aspect.

With the work presented here, we succeeded for the first time in demonstrating the strong influence of ion-pair effects on the

(24) Kaupp, G.; Laarhoven, W. H. *Tetrahedron Lett.* **1976**, 941.
(25) Yamashita, Y.; Yaegashi, H.; Mukai, T. *Tetrahedron Lett.* **1985**, 3579.
(26) Hall, D. M.; Leslie, M.; Turner, E. *J. Chem. Soc.* **1950**, 711.
(27) Müllen, K.; Huber, W.; Meul, T.; Nakagawa, M.; Iyoda, M. *J. Am. Chem. Soc.* **1982**, *104*, 5403. Müllen, K.; Meul, T.; Schade, P.; Schmickler, H.; Volge, E. *J. Am. Chem. Soc.* **1987**, *109*, 4992. Becker, B. C.; Huber, W.; Schnieders, C.; Müllen, K. *Chem. Ber.* **1983**, *116*, 1573.

mechanism and the kinetics of charge-transfer-induced valence isomerizations.

From the mechanistic point of view, it seems to be interesting that the intramolecular bond formation takes place even at the di- and triionic level. This is comparable with a radical–radical coupling (RR route). The nucleophilic attack of an olefinic radical anion on the double bond of a second neutral olefin, the so-called RS route (radical–substrate coupling), has been postulated in the literature[28] as a mechanistic variant for hydrodimerization reactions, but has not been experimentally proved nor excluded. The experiments presented here are evidence that RS coupling is generally improbable for ionic dimerization reactions.

5. Experimental Section

The ESR spectra of the paramagnetic radical anions $\mathbf{1}^{\bullet-}$ were measured with a Bruker ESP 300 spectrometer. ^{1}H and ^{13}C NMR spectra were obtained using a Bruker AM 200 spectrometer. Mass spectra were recorded on a Varian MAT CH7A instrument. The simulation of the benzylic ABX spin system of **6** was performed with the help of the Bruker program PANIC, Version 85051.

All solvents used were distilled and, if necessary, dried and degassed. The absolute THF used for the reduction experiments was distilled twice under argon from potassium/benzophenone.

Electrochemical Measurements. Our standard electrochemical instrumentation consisted of a PAR Model 173 potentiostat/galvanostat and a PAR Model 175 universal programmer. Cyclic voltammograms were recorded with a Philips Model PM8131 X-Y-recorder. A three-electrode configuration was employed throughout. The working electrode was a Pt disk (diameter 1 mm) sealed in soft glass. The counter electrode was a Pt wire coiled around the glass mantle of the working electrode. The reference electrode was a simple Ag wire for the measurements in DMA and, for the measurements in THF, a Ag wire on which AgCl had been deposited electrochemically, immersed in the electrolyte solution. Potentials were calibrated against the formal potential of ferrocene (+0.35 V vs Ag/AgCl) in the case of THF and against cobaltocenium perchlorate (−0.94 V vs Ag/AgCl) in the case of DMA. All manipulations were carried out under an argon atmosphere.

Synthesis of the Title Compounds 1 and 5. 2,2′-Distyrylbiphenyl (1). The synthesis of **1** was carried out according to the method developed by Hall et al.[26] The last step, a two-fold Wittig reaction between bis(methyltriphenylphosphonio)biphenyl dibromide and benzaldehyde, was modified according to Tulloch and Kemp.[12] From the isomeric mixture obtained in this reaction, the trans,trans isomer of **1**, which was used exclusively for the following examinations, could be isolated through repeated recrystallization from absolute methanol in 20% yield: mp 147 °C; ^{1}H NMR (200 MHz, $CDCl_3$) δ 7.80 (m, 2 H), 7.24 (m, 16 H), 6.92 (AB, 4 H); ^{13}C NMR (50 MHz, $CDCl_3$) δ 140.1, 137.8, 136.3, 131.1, 129.8, 128.6, 127.9, 127.6, 127.5, 127.3, 126.6, 125.4; MS *m/e* 265 (16, M − C_7H_9), 252 (13, M − C_8H_{10}), 180 (69, stilbene), 178 (100, phenanthrene).

2,2′-Bis(3″,5″-di-*tert*-butylstyryl)biphenyl (5). (4.6 g, 22 mmol) Diphenic dialdehyde and 25.1 g (46 mmol) of (3,5-di-*tert*-butylbenzyl)triphenylphosphonium bromide dissolved in 200 mL of boiling ethanol were added under argon over 4 h to a 0.4 M NaOEt solution in the same solvent. After 30 min, the solvent was evaporated. The residue was treated with water and extracted with methylene chloride, the organic layer was dried over $MgSO_4$, and the solvent was removed under reduced pressure. The raw product was chromatographed on silica gel (methylene chloride/petroleum ether 5:1). The isomeric mixture of **5**, a colorless oil, was isomerized with iodine in boiling toluene. Through fractionated low-temperature crystallization from absolute methanol the trans,trans isomer **5** (3.88 g, 30%) could be isolated as colorless plates: mp 127–128 °C; ^{1}H NMR (200 MHz, $CDCl_3$) δ 7.83 (d, 2 H), 7.36 (m, 8 H), 7.13 (s, 4 H), 7.00 (AB, 4 H), 1.27 (s, 36 H); ^{13}C NMR (50 MHz, $CDCl_3$) δ 150.8, 140.1, 137.2, 136.5, 131.0, 130.4, 127.8, 127.5, 127.1, 124.9, 121.8, 121.0, 34.8, 31.5; MS *m/e* 582 (0.08, M^+), 404 (87, M − $C_{14}H_{12}$), 178 (4, phenanthrene), 57 (100, C_4H_9).

Reduction Experiments under Spectroscopic Control. The neutral compounds **1** and **5** were converted into their anions via reduction with highly active lithium or potassium metal. Details of the preparation technique have been described elsewhere.[27]

Preparative Reductions in THF. The alkali metal reductions of **1** under heterogeneous conditions were carried out in a special two-chambered ampoule. After a degassed solution of 80 mg (0.22 mmol) of **1** in 20 mL of absolute THF was placed in the lower chamber, the necessary amount of lithium in the form of highly active wire (or potassium metal vapor-deposited on the glass walls) was introduced into the second chamber. Thereafter, the ampoule was sealed, brought to the appropriate reaction temperature, and the reaction solution was contacted with the metal. During the course of the reduction the solution turned dark. The reaction was finished when all of the potassium went into solution or the chosen time of contact was reached. The reaction solution was separated from excess metal by turning the reaction vessel. The ampoule was opened under argon, and the quenching agent was added in a gas counterflow. The quenching process was complete when the reaction solution had lost all color. Depending on the quenching agent, this process took from a few seconds up to 45 min. The product mixtures were chromatographed on silica gel. As eluting agents, petroleum ether/methylene chloride mixtures were used. With increasing solvent polarity, phenanthrene, stilbene, their protonation products, starting material **1**, **10**, cyclobutane derivative **2**, dihydrophenanthrene derivative **6**, and finally oligomers or polymers were eluted. The *tert*-butyl-substituted substrate **5** was reacted and purified in an analogous manner.

For the homogeneous reduction using an organic mediator, glass ampoules with a third chamber were employed. In the two-chamber part of the ampoule, a stoichiometric amount of the mediator was contacted as described above with lithium and transformed quantitatively into its dianion. After separating the excess alkali metal, half of the solvent was condensed into the third chamber in which the substrate was dissolved, and both solutions were combined by swinging the ampoule. After a fixed reaction time, workup followed as described above. The mediators and the protonation products were eluted from the column first and the dihydroanthracene adduct **11** directly after the DHP derivative **6**.

11: ^{1}H NMR (200 MHz, $CDCl_3$) δ 7.81 (m, 1 H), 7.64 (d, 1 H), 7.44 (m, 5 H), 7.26 (m, 2 H), 7.10 (m, 2 H), 6.83 (m, 8 H), 6.59 (m, 3 H), 6.02 (bs, 1 H), 5.53 (bs, 1 H), 4.58 (bs, 1 H), 4.04 (q, 1 H), 3.34 (d, 1 H), 3.09 (d, 1 H), 2.87 (dd + d, 2 H), 2.64 (d + d, 1 H), 1.86 (d, 1 H); MS *m/e* 537 (2, M + 1^+), 536 (4, M^+), 268 (67, M − anthracene − C_7H_6), 267 (67, M − anthracene − C_7H_7), 191 (32, $C_{15}H_{11}$), 178 (41, anthracene + phenanthrene), 91 (100, C_7H_7).

Preparative Reductions in Ammonia/THF; Synthesis of *trans*-9,10-Dibenzyl-9,10-dihydrophenanthrene (6). Compound **1** (200 mg, 0.55 mmol) was dissolved in 40 mL of absolute THF, degassed, and cooled to −50 °C. At this temperature, 40 mL of sodium-dried ammonia were condensed into the flask, and the necessary amount of oxide-free potassium was added. The alkali metal dissolved within several minutes, while the reaction mixture took on the brown color of the substrate anion. The reaction was allowed to continue for some time (refer to Table II); in other cases the cosolvent ammonia was evaporated quickly. The chosen quenching agent was added and, after the reaction mixture had decolorized completely, solid ammonium chloride was added. The reaction mixture was then allowed to warm to room temperature. Water was added, the aqueous layer extracted with methylene chloride, the organic layer dried over $MgSO_4$, and the crude product chromatographed as described above. Depending on the reaction conditions, varying amounts of the DHP derivative **6** were isolated in the form of a viscous oil (see Table II): ^{1}H NMR (200 MHz, $CDCl_3$) δ 7.88 (d, 2 H), 7.35 (m, 2 H), 7.18 (m, 8 H), 6.96 (d, 2 H), 6.85 (m, 4 H), 2.98 and 2.58 (ABX, 6 H, δ_A = 2.50, δ_B = 2.65, δ_X = 2.97, J_{AB} = −13.41 Hz, J_{AX} = 8.57 Hz, J_{BX} = 6.31 Hz, determined by simulation); ^{13}C NMR (50 MHz, $CDCl_3$) δ 140.0, 138.2, 132.9, 129.9, 129.1, 128.0, 127.6, 127.2, 123.7, 44.6, 41.0; MS *m/e* 360 (4, M^+), 269 (21, M − C_7H_7), 178 (28, phenanthrene), 91 (100, C_7H_7).

Thermolysis of 1. Compound **1** (100 mg, 0.27 mmol) was placed in a dry NMR tube, which was flushed with argon and heated in a metal bath to 240–250 °C for 2 h. After cooling, the product mixture formed was washed from the tube with methylene chloride and separated by column chromatography. Besides 30% phenanthrene and stilbene, 39% (39 mg) of the cyclobutane derivative **2a** was isolated as a colorless oil, which crystallized upon standing: mp 167 °C; ^{1}H NMR (200 MHz, $CDCl_3$) δ 7.97 (d, 2 H), 7.20 (m, 16 H), 4.20 (AA′BB′, 4 H).

Photolysis of 1. In a commercial photoreactor equipped with a high-pressure mercury lamp (Philips HPK, 125-W) and a Pyrex filter, a solution of **1** (107 mg, 0.3 mmol) was irradiated in 300 mL of degassed hexane while stirring. After the solvent was removed and the crude product was recrystallized from methanol, the cyclobutane derivative **2b** was isolated in a yield of 92% (98.4 mg): mp 129 °C; ^{1}H NMR (200 MHz, $CDCl_3$) δ 7.83 (d, 2 H), 7.30 (m, 16 H), 3.51 (AA′BB′, 4 H).

Acknowledgment. We gratefully acknowledge the Volkswagen-Stiftung, the Deutsche Forschungsgemeinschaft, and the Fonds der Chemischen Industrie for financial support of this work.

(28) Figeys, M.; Figeys, H. P. *Tetrahedron* **1968**, *24*, 1097.

Registry No. 1, 33510-35-9; $\mathbf{1}^{\bullet-}$, 67463-61-0; $\mathbf{1}^{2-}$, 137571-24-5; $\mathbf{1}^{\bullet3-}$, 137624-71-6; $\mathbf{1}^{4-}$, 137571-25-6; **2b**, 38385-44-3; $\mathbf{2b}^{\bullet-}$, 137624-70-5; $\mathbf{3}^{2-}$,

137571-28-9; $3^{\cdot 3-}$, 137693-20-0; **5**, 137571-19-8; $5^{\cdot -}$, 137624-72-7; 5^{2-}, 137571-26-7; $5^{\cdot 3-}$, 137624-73-8; 5^{4-}, 137571-27-8; $5^{4-}/4Li^{+}$, 137571-18-7; **6**, 137571-20-1; $6^{\cdot -}$, 137624-74-9; **7a**, 137571-21-2; **7b**, 137571-22-3; **8**, 137571-23-4; $8^{\cdot -}$, 137624-75-0; **10**, 4284-01-9; **11**, 137594-02-6; 12^{2-}, 137571-29-0; TBABr, 1643-19-2; $TBAPF_6$, 3109-63-5; K, 7440-09-7; $CdCl_2$, 10108-64-2; $C_3H_6Br_2$, 109-64-8; I_2, 7553-56-2; MeOH, 67-56-1; diphenic dialdehyde, 1210-05-5; (3,5-di-*tert*-butylbenzyl)triphenylphosphonium bromide, 36393-44-9; lithium, 7439-93-2; anthracene, 120-12-7; stilbene, 588-59-0; lithium tetraphenylborate, 14485-20-2; sodium tetraphenylborate, 143-66-8; 15-crown-5, 33100-27-5.

Ionization of Purine Nucleosides and Nucleotides and Their Components by 193-nm Laser Photolysis in Aqueous Solution: Model Studies for Oxidative Damage of DNA[1]

L. P. Candeias and S. Steenken*

Contribution from the Max-Planck-Institut für Strahlenchemie, D-4330 Mülheim, Germany.
Received July 1, 1991. Revised Manuscript Received September 9, 1991

Abstract: The effect of 20-ns pulses of 193-nm laser light on aqueous solutions of purine bases, (2′-deoxy)nucleosides, and (2′-deoxy)nucleotides was investigated, and monophotonic ionization was observed. Although (deoxy)ribose and (deoxy)ribose phosphates are also ionized by 193-nm light, the photoionization of the (deoxy)nucleosides and -tides takes place predominantly (90%) at the purine moiety, due to the much higher extinction coefficients at 193 nm of the bases as compared to the (deoxy)ribose phosphates. The quantum yields of photoionization (ϕ_{PI}) of the purines are in the range 0.01 to 0.08, based on $\phi_{PI}(Cl^-)$ at 193 nm of 0.46. As shown by comparison with data obtained from pulse radiolysis, the ionized purines, i.e., the radical cations, deprotonate in neutral solution, yielding neutral radicals. The radical cation of 1-methylguanosine, produced by photoionization in oxygen-saturated aqueous solution, deprotonates with the rate constant 3.5×10^5 s^{-1}. In the absence of oxygen, the hydrated electrons resulting from the photoionization react with the untransformed purine derivatives to yield the corresponding radical anions. As these are rapidly protonated by water (as concluded from pulse radiolysis), the photoionization in deaerated neutral solution results in two different neutral radicals: a *deprotonated* radical cation and a *protonated* radical anion.

Introduction

The chemical and biological effects of UV radiation on DNA or its constituents have been the subject of numerous studies.[2] However, these have mostly involved the use of light with wavelengths of ~250 nm. With the energies corresponding to these wavelengths, the *ionization* of purines (gas-phase ionization potentials ≳8 eV)[3] with only *one* photon is thermodynamically barely possible and is essentially not observed (with one 248-nm photon corresponding to 4.9 eV and the solvation energies of the ions formed being ≲3.5 eV,[4] ionization would at best be thermoneutral). The reported[2,5-9] ionizations of nucleic acid bases on interaction with ~250-nm light are therefore due to multiphotonic, usually biphotonic, processes, the yields of which depend, by definition, on the intensity of the exciting light.

However, with 193-nm light as emitted by argon fluoride excimer lasers, *mono*photonic ionization of purines (and pyrimidines) should be possible since ≲9.9 eV is available (the 193-nm quantum energy contributes 6.4, and there is ≲3.5 eV from the hydration of the ions produced). An advantage of 193-nm light compared to that of shorter wavelengths is that it is above the onset of light absorption by H_2O (~180 nm). This means that complications due to the formation of H· and OH· radicals are avoided.

UV light of wavelength 193 nm has already been used to excite DNA[10-12] or its bases.[8] With the latter, evidence for the occurrence of ionization was in fact obtained,[8] but the resulting radicals were not identified nor were any data given to judge the importance of ionization relative to other, *non*ionic photochemical processes. In the studies on the effect of ~190-nm light on DNA,[10-12] the interesting observation was made[10,11] that the type of damage produced is different from that observed[13] with low-intensity ~250-nm light but similar to that[14] with ionizing radiation. If

(1) Preliminary reports of this work were given at the 11th GdCh Photochemistry Meeting at Duisburg, 22–24 November 1989. See also: Candeias, L. P.; Steenken, S. *Int. J. Radiat. Biol.* **1990**, *58*, 889.

(2) For recent reviews, see: (a) Cadet, J.; Vigny, P. In *Bioorganic Photochemistry, Vol. 1, Photochemistry and the Nucleic Acids*; Morrison, H., Ed.; Wiley: New York, 1990; p 1. (b) Nikogosyan, D. N. *Int. J. Radiat. Biol.* **1990**, *57*, 233. (c) Schulte-Frohlinde, D.; Görner, H.; Simic, M. G. *Photochem. Photobiol.* **1990**, *52*, 1137.

(3) Orlov, V. M.; Smirnov, A. N.; Varshavsky, Y. M. *Tetrahedron Lett.* **1976**, 4377.

(4) Braun, M.; Fan, J. Y.; Fuss, W.; Kompa, K. L.; Müller, G.; Schmid, W. E. In *Methods in Laser Spectroscopy*; Prior, Y., Ben-Reuven, A., Rosenbluh, M., Eds.; Plenum Press: New York, 1986; p 367.

(5) Görner, H. *Photochem. Photobiol.* **1990**, *52*, 935. Bothe, E.; Görner, H.; Opitz, J.; Schulte-Frohlinde, D.; Siddiqi, A.; Wala, M. *Photochem. Photobiol.* **1990**, *52*, 949.

(6) Arce, R. *Photochem. Photobiol.* **1987**, *45*, 713. Arce, R.; Rivera, J. *J. Photochem. Photobiol.* **1989**, *A49*, 219. Quinones, E.; Arce, R. *J. Am. Chem. Soc.* **1989**, *111*, 8218.

(7) (a) Sevilla, M. D. *J. Phys. Chem.* **1971**, *75*, 626. (b) Sevilla, M. D.; van Paemel, C.; Nichols, C. *Ibid.* **1972**, *76*, 3571.

(8) Kasama, K.; Takematsu, A.; Arai, S. *J. Phys. Chem.* **1982**, *86*, 2420.

(9) Croke, D. T.; Blau, W.; OhUigin, C.; Kelly, J. M.; McConnell, D. J. *Photochem. Photobiol.* **1988**, *47*, 527.

(10) Johnson-Thompson, M.; Halpern, J. B.; Jackson, W. M.; George, J. *Photochem. Photobiol.* **1984**, *39*, 17.

(11) Kochevar, I. E.; Buckley, L. A. *Photochem. Photobiol.* **1990**, *51*, 527.

(12) Ito, T.; Sutherland, J. C. *Photochem. Photobiol.* **1986**, *44*, 235. Hieda, K.; Hayakawa, Y.; Ito, K.; Kobayashi, K.; Ito, T. *Ibid.*, 379. Takakura, K.; Ishikawa, M.; Hieda, K.; Kobayashi, K.; Ito, A.; Ito, T. *Ibid.*, 397. Green, H. A.; Boll, J.; Parrish, J. A.; Kochevar, I. E.; Oseroff, A. R. *Cancer Res.* **1987**, *47*, 410.

(13) For reviews see, for example: Patrick, M. H.; Rahn, R. O. In *Photochemistry and Photobiology of Nucleic Acids*; Wang, S. Y., Ed.; Academic: New York 1976; Vol. II, p 35. Rahn, R. O.; Patrick, M. H. *Ibid.*, p 97.

(14) For reviews see, for example: Hüttermann, J., Köhnlein, W., Téoule, R., Bertinchamps, A. J. Eds.; *Effects of Ionizing Radiation on DNA*; Springer-Verlag: Berlin, 1978.

0002-7863/92/1514-699$03.00/0 © 1992 American Chemical Society